Title: Role of spheroidal particles in closure studies for aerosol microphysical-optical properties

Author(s): Sorribas, M., Olmo, F.J., Quirantes, A., Lyamani, H., Gil-Ojeda, M., Alados-Arboledas, L., Horvath, H.

Source: Quarterly Journal of the Royal Meteorological Society, 2015, DOI: 10.1002/qj.2557

ROLE OF SPHEROIDS PARTICLES ON CLOSURE STUDIES FOR AEROSOL MICROPHYSICAL-OPTICAL PROPERTIES

Sorribas, M.[1,2], Olmo, F.J.[1,2], Quirantes, A.[1], Lyamani, H.[1,2], Gil-Ojeda, M.[3], Alados-Arboledas, L.[1,2], Horvath, H.[4]

1. Department of Applied Physics, University of Granada, Granada, 18071, Spain

2. Andalusian Institute for Earth System Research (IISTA), University of Granada, 18006, Spain

3. Atmospheric Research and Instrumentation Branch, INTA, Madrid, 28850, Spain

4. Faculty of Physics, University of Vienna, Vienna, 1090, Austria

Corresponding author: Mar Sorribas (sorribas@ugr.es)

Running head: Spheroids particles on closure studies

ABSTRACT

A study has been carried out to assess the discrepancies between computed and observed aerosol scattering and backscattering properties in the atmosphere. The goals were: (1) to analyze the uncertainty associated with computed optical properties when spherical and spheroid approximations are used and (2) to estimate nephelometry errors due to angular truncation and non-Lambertian illumination of the light source in terms of size range, particle shape and aerosol chemical compounds. Mie and T-matrix theories were used for computing light optical properties for spherical and spheroid particles, respectively, from observed particle size distributions. The scattering coefficient of the fine mode was not much influenced by the particle shape. However, computed backscattering values underestimated the observed values by ~ 15%. For the coarse mode the spheroidal approximation yields better results than that for spherical particles, especially for backscattering properties. Even after applying the spheroidal approximation, computed scattering and backscattering values within the coarse mode underestimated the observed values by ~49% and ~11%, respectively. The angular correction most widely used to correct the nephelometer data was discussed to explore its uncertainty. In the case of the scattering properties within the coarse mode the change of the computed optical parameter is ~+8% and for the scattering and backscattering values within the fine mode it is lower than ~±4% for spherical and spheroid particles. Additionally, if the spheroid particles are used to evaluate the aerosol optical properties, the correction must be reconsidered with the aim of reducing the uncertainty found for scattering within the coarse mode. This is recommended for sites with desert dust influence, then the deviation of the computed scattering can be up to 13%.

Keywords: atmospheric aerosol, spheroidal particles, spherical particles, aerosol microphysical properties, aerosol optical properties

1. INTRODUCTION

Natural and anthropogenic particles in the atmosphere alter the Earth's energy budget and are drivers of climate change. Aquantification of energy fluxes via radiative forcing can be estimated based on either in-situ observations, remote sensing, or computations by numerical models which represent the aerosol-radiation interaction (IPCC, 2014). A full description of the interaction of the solar radiation in the atmosphere, within reach of modern theories, is possible. The process is described via the radiative transfer equation; algorithms for solving the radiative transfer exist, but the more precise computing resources are needed. With respect to the input, a full description of the aerosol optical properties in 3 dimensions is needed and is usually not available, which calls for restricting assumptions.

Real aerosol particles rarely exhibit spherical shapes, but rather have more complex geometry. Some examples of non-spherical particles are volcanic ash, desert dust and sea salt particles. Mie theory (Mie, 1908) yields optical properties for the case of homogeneous spheres. For non-spherical particles a number of light scattering theories have been developed (Mishchenko and Travis., 1998; Dubovick et al., 2002). In studying theoretical scattering properties of atmospheric particles, which always are polydispersed, two important facts should be considered: (a) the particle's non-sphericity, which is known to have a great impact on the large uncertainties in the Earth's climate (Kahnert et al., 2007; Raisanen et al., 2013) and (b) uncertainties associated with instruments for measuring microphysical and optical aerosol properties, which also depend on particle shape (Anderson and Ogren, 1998; Müller et al., 2011).

Regarding the uncertainty of optical properties due to spherical and non-spherical approximations, in this paper we shall present examples simulating particle scattering and backscattering properties from observed particle size distributions, which are compared with observational optical data. This analysis is performed for different size ranges: particles with

diameters lower than 1 μm (fine mode) and those with diameters within (1-10) μm (coarse mode). The relationship between computed and observed optical data will be described from two points of view: (a) analyzing the computed properties when spherical and non-spherical approximations are considered, and (b) considering different aerosol sources distinguishing data influenced by desert dust and non-desert dust.

Regarding uncertainties associated with instrumentation, we shall present an investigation of the TSI's integrating nephelometer (Model 3563), an instrument widely used to measure the aerosol scattering and backscattering properties (Anderson et al., 1998; Müller et al., 2011). Ideally it should integrate light scattered by the particles in a volume of air over a full 0º - 180º angular range. All these directions are required for accurately study the aerosol scattering properties. In reality the light scattered in the near-forward (0º to 7º) and near-backward directions (170º to 180º) directions cannot be measured, causing a systematic uncertainty of the integrating nephelometry technique. This limitation is commonly known as the angular truncation error. Additionally, the illumination function of the nephelometer light source deviates little from a Lambertian radiant emission (Anderson et al., 1996), meaning that the angular illumination of the particles is almost a sine-function. One of the most popular corrections for both deviations (non-Lambertian illumination and the angular truncation) was presented by Anderson and Ogren (1998), and its uncertainty is analyzed in our work. In the following sections, the term 'angular correction' comprises both corrections and the term 'angular sensitivities' is related to the illumination and angular truncation functions, which have been applied on the Mie and T-matrix codes.

The paper is organized as follows: Section 2 describes the experimental devices used to measure the light scattering and backscattering properties and the particle number size distribution. The methodologies applied to the computation of optical properties using the Mie model and T-

matrix method are shown in Section 3, as well as the definition of the angular correction. The results are reported in Section 4. In Section 4.1., the analysis of the spherical and non-spherical approximations is carried out and compared to observational data. The uncertainty study on the angular correction is given in Section 4.2. These latter analyses are presented in terms of different aerosol sources, which were classified into desert and non-desert dust air mass origins.

2. EXPERIMENTAL DEVICE

'El Arenosillo' Atmospheric Sounding Station is situated in a protected rural environment (Doñana National Park), in South-western Spain (37.1°N, 6.7°W, 40 m a.s.l.), on the coast of the Atlantic Ocean and close to the North African coast. This observatory submits data to the World Ozone and Ultraviolet Radiation Data Centre (WOUDC) and World Data Centre for Aerosols (WDCA) of the Global Atmosphere Watch (GAW) program at the World Meteorological Organization (WMO). The monitoring, retrieval and reporting procedures are standardized by the WMO quality assurance methodology. More information regarding this observatory is available in several references (e.g. Prats et al., 2008; Córdoba-Jabonero et al., 2011; Guerrero-Rascado et al., 2011; Anton et al., 2012; Adame et al., 2014; Sorribas et al., 2011; 2015a; 2015b).

The multi-instrumental study of aerosol properties was carried out at El Arenosillo Station (Southwest Spain) from May to September 2009. The sub-micron and super-micron particle size distributions were assumed to be ($D<1$ μm) and (1 μm $<D<10$ μm), respectively. The interval of the dry ambient sub-micron size distribution was monitored by a Scanning Mobility Particle Sizer (SMPS) (Electrostatic Classifier TSI Mod. 3080 and a Condensation Particle Counter TSI Mod. 3776). The SMPS dataset was corrected for losses caused by diffusion processes and multiple charges inside the instrument. The uncertainties of the measured size distributions are assumed to be ±10% from 20 to 200 nm while above this size range it increases to 30%

(Wiedensohler et al., 2012). The dry ambient super-micron size distributions within (1-10) μm were monitored by an Aerodynamic Particle Sizer (APS) (TSI Mod. 3321) in summing mode. The APS error due to particle density higher than 1 g c m^{-3} was corrected using the Stokes particle density correction (Wang and Walter, 1987). The uncertainty of the APS is approximately ±10%. The sampling system efficiency was calculated according to Willeke and Baron (1993) and was 98% for the [0.0165-1] μm particle mobility diameter range and ranged from 98% for 1 μm to 50 % for 10 μm. Sample flows for SMPS and APS were dried to RH< 30% using a Nafion dryer (Perma Pure Inc., Toms River, N) by supplying under-pressured dry air to the sheath of the dryer. AIM software (version 9.0.0., TSI INC., St Paul., MN, USA) was used for SMPS and APS output data reduction and analysis. The Q-assumption describes the dependence of the aerodynamic volume size distribution on the particle density and the shape factor (more details in Sorribas et al., 2015a). It was used to convert the aerodynamic diameter measured by the APS system to the mobility diameter to make comparable the SMPS and APS data.

An integrating nephelometer (TSI Mod. 3563) was used for the integrated scattering (σ_{sp}) and backscattering (σ_{bsp}) particle measurements, measuring the scattered light through bandpass filters at the 450 nm, 550 nm and 700 nm wavelengths with a bandwidth of 40 nm (all wavelengths). This nephelometer works under the framework of the NOAA/ESRL aerosol Network (http://www.esrl.noaa.gov/gmd/aero/net/arn/index.html), where the measurements are corrected for known instrumental non-idealities (e.g., Anderson and Ogren, 1998). The uncertainties of the measured scattering and back-scattering are assumed to be ±10%. A span check of the nephelometer was carried out every week using CO_2 and dry-filtered air, and a zero signal was measured every hour. A switched impactor system provided the size-segregated aerosol light scattering. The nephelometer measured the light scattering by aerosols smaller than 10-μm aerodynamic diameter through the use of a Thermo PM10 inlet located outside the

laboratory. Every 5 min, a valve was opened or closed to measure the alternating sub-micron (D < 1 μm) and sub-plus-super-micron (D < 10 μm) size ranges. When the valve was closed, the aerosol passed through an impactor having 1-μm aerodynamic cut-point. In this study, only datasets with relative humidity values lower than 60 % were used. In this way the relative humidity had a mean value of 48±8 %. The uncertainty on the optical parameters due to changes in RH inside the nephelometer is higher than in the SMPS and APS measurements and it was estimated to be less than +5% at RH=60% (Sorribas et al., 2015a).

3. METHODOLOGY

The EBCM, or T-matrix (Mishchenko, 1991) theory has been used to calculate light scattering properties for non-spherical particles. Both incident and scattered electric fields can be expanded in vector spherical wave functions. Incident and scattered expansion field coefficients can be related by means of a transition (T) matrix, whose elements depend on the particle size, shape and orientation. In the case of randomly oriented, axially symmetric particles, the T-matrix is calculated for the natural reference frame (z-axis along the particle symmetry axis) and results are then averaged for all particle orientations. In order to model non-spherical particles, they will be represented as a collection of scatterers with a symmetry plane (e.g. spheroids).

The use of T-matrix data in collections of polydisperse particles can be cumbersome and time-consuming. To alleviate this problem, light-scattering properties can be approximated as a sum of kernel functions K (Dubovik et al., 2006):

$$\tau_{sca}(\lambda) \approx \frac{2\pi}{\lambda} \sum_{p=1}^{N_p} \sum_{l=1}^{N_l} \frac{dV(r_p)}{d\ln r} \frac{dN'(e_l)}{d\ln e} K_{sca}(m, x_p, e_l) \quad (1)$$

Kernel functions depend on the index of refraction (m), size (x_p) and shape (e_i) parameters. A pre-calculated set of kernel functions ("BETA" database) was shown in (Quirantes et al., 2010; 2011) and it was already used in previous studies (Quirantes et al., 2012; Valenzuela et al., 2012a; 2012b; 2012c)

In the present study, particles are modelled as prolate and oblate spheroids with an eccentricity parameter ε and an axial ratio e (long-to-short axis ratio): ε=e for oblate spheroids, and ε=1/e for prolate spheroids. Previous studies (i.e. Hill et al., 1984; Mishchenko et al., 1997) modelled light scattering properties of real and non-spherical atmospheric aerosols by a particle distribution of prolate and oblate spheroids (50% in volume) with an axial ratio e = 1.8. This model configuration will be also used in our work. About the size parameter, x_p is a dimensionless parameter, which is evaluated by x = kr, where r value is the radius of the equal-volume sphere and k value is the wavenumber, $k = 2\pi/\lambda$, being λ the wavelength. In the cases where particles can be assumed to be spherical, Mie theory has been used (Mie, 1908). On the other hand, in our computations (spherical and spheroid approximations) the nephelometer nonidealities - wavelength and angular sensitivities - (Anderson et al., 1996) are considered.

The integrating nephelometer is the instrument most widely used to measure the light scattering by aerosols. As the integrating nephelometer is included as part of the instrumental setup in the aerosol program of the World Meteorological Organization (WMO), an effort to improve the accurate measurement of total scattering was carried out over the last few decades (e.g. Bond et al., 2009; Massoli et al., 2009). An important measurement limitation of the nephelometer instrument, the angular truncation error, is that light scattered at angles smaller than ~7º and larger than ~170º is neglected. Additionally, a second limitation is the non-Lambertian radiant emission of the nephelometer light source. The deviation in the measured scattering produced by both angular deviations is lower than 10% within the fine mode, increasing up to 20% within the coarse mode. For backscattering there is no dependence on particle size, and the error is less than

10% (Anderson et al., 1996). Other authors found higher deviations, e.g., Heintzenberg et al. (2006), who showed that for size distributions of geometric mean diameters up to 2 μm, up 35% of the scattered light is not measured due to angular deviations. Taking into account that high uncertainty levels are to be expected if the integrating nephelometer has a poorly characterized angular truncation response, a correction factor was developed to reduce such errors (Anderson and Ogren, 1998). The truncation correction, C_{ts}, is defined as,

$$C_{ts}(\lambda) = \frac{\sigma_{sp,Mie}(\lambda)}{\sigma_{sp,neph}(\lambda)} \tag{2}$$

where $\sigma_{sp,Mie}$ is the true particle scattering computed by Mie theory and $\sigma_{sp,neph}$ is the particle scattering measured by the nephelometer. The angular scattering varies with particle size and therefore the angular correction also depends on particle diameter. The optical parameter related to both the wavelength dependence of scattering and the average particle size is the Ångström exponent (å) for scattering.

$$\text{å} = -\frac{\ln((\sigma_{sp}(\lambda_1)/\sigma_{sp}(\lambda_2))}{\ln(\lambda_1/\lambda_2)} \tag{3}$$

Based on the calculated Ångström exponent, the angular correction is evaluated as $C_{ts}=(a+b\cdot\text{å})$, as Table 1 shows. The pairs of wavelength values used to calculate the Ångström exponent are (450-550) nm, (450-700) nm and (550-700) nm to correct σ_{sp}(450 nm), σ_{sp}(550 nm) and σ_{sp}(700 nm) respectively.

In the case of backscattering, the angular correction is assumed to be independent of particle size, with values of 0.981, 0.982 and 0.985 at 450, 550 and 700 nm wavelengths, respectively.

This widely used correction has been studied previously in terms of its impact on other aerosol parameters. For example, Bond et al. (2009) showed that using of this angular correction, absorption, single-scattering albedo and negative forcing is overestimated by about (1-5)%. In Massoli et al. (2009), a higher overestimation was found for a single-scattering albedo values higher than 0.7, concluding that this is mostly due to the higher real part of the refractive index of the absorbing material.

4. RESULTS

4.1. Shape approximations in the computed optical properties

To clarify the differences between the use of spherical and non-spherical models in closure studies, observed σ_{sp} and σ_{bsp} were compared with computed values using both shapes. In this section, computed and observed optical properties were compared with the light scattered in the (7º-170º) angle range. The computed properties were calculated using the wavelength and angular sensitivities (Anderson et al., 1996). The Anderson and Ogren, (1998) correction was not applied on the observed properties. Using the SMPS-APS measured number size distributions, Mie and T-matrix Methods were used to calculate the optical properties (σ_{sp} and σ_{bsp}) at wavelengths of 450 nm, 550 nm and 700 nm. In the present work, the comments refer to the 550 nm wavelength, although all wavelengths are shown in the Figures. The σ_{sp} value was calculated with hourly averages of the SMPS-APS data and refractive index (m) values of 1.482 and 1.527 were estimated for fine and coarse modes, respectively. The calculation of m was performed using the volume-weighted method (Hand and Kreidenweis, 2002) and experimental chemical compounds information. More details about the refractive indices used for the particle composition are given in Sorribas et al. (2015a).

For particles with D < 1 μm (fine mode), Figures 1a compare the computed and observed scattering coefficients and Figures 1b compare the backscattering values at 450 nm, 550 nm and 700 nm. Results suggest a strong correlation between computed and observed values for spherical (black dots) and spheroidal (red dots) particles and, hence, good agreement between the optical and microphysical aerosol properties. High correlation coefficients (R=0.91-0.97) were found for all wavelengths. The largest difference between the observed and calculated optical properties by spherical particles is associated with the slope of the fit, in the range of 0.87-0.96 for scattering and 0.73-0.87 for backscattering. Therefore, while the computed scattering values lie within ~ ±10% of the uncertainties of the observed scattering (see Section 2), an underestimation of the computed backscattering values is evident. The lowest slopes of the fit were for the largest wavelengths. On the other hand, the scattering properties for spheroid particles decrease the slope by about 3% compared to the slope for spherical particles, while for backscattering there are no differences. For this reason, for use in climate models the assumption of either spherical or spheroidal particles for fine particles would not cause a change in the observed findings.

For particles with 1 μm < D < 10 μm (coarse mode), a comparison between calculated and observed scattering values is shown in Figures 1c, and Figures 1d compare the backscattering values at the three wavelengths. Good correlation is observed, but the correlation coefficient (R) ranged from 0.72 to 0.85 and is lower than for the fine mode. The Mie theory computations for spherical particles underestimate the scattering coefficients by 54% (slope of the fit with a value of 0.46) at 550 nm. The backscattering value underestimation of about 53% at 550 nm is similar than that of scattering. In both scattering and backscattering, the underestimation becomes less important with increasing wavelength. Previous ground-based scattering closure studies showed that the differences between observed and computed values (coarse mode) can be attributed to the effect of non-spherical particles (e.g., Marshall et al., 2007; Chen et al., 2011). In our work,

this effect is analyzed by computation of the T-matrix Method. The computed scattering and backscattering values assuming spheroidal particles still underestimate the observed values, but with better results. Thus, the underestimations of σ_{sp} and σ_{bsp} at 550 nm are 49% and 11% (slopes of the fit with values of 0.51 and 0.89), respectively. Therefore, the spheroid approximation has greater impact on backscattering than on scattering within the coarse mode. In general, underestimation of scattering and backscattering by spheroidal particles becomes less important with increasing wavelength, similar to the case of spherical particles.

Ideally, model particles should be representative for the real (observed) particles in all characteristics relevant for scattering and backscattering, and therefore the slope of the fit should be 1. However, even after applying the spheroids approximation, the computed optical parameters underestimate the observed properties within the coarse mode. If the inherent limitations of modelling scattering and backscattering methods are neglected, this underestimation may be due to uncertainty in particle modelling either (i) spheroid geometry (axial ratio) (Klaver et al., 2011) or (ii) particle composition (refractive index) (Lindqvist et al., 2014), as well as uncertainty in the particle size distribution measurement.

Taking into account the fact that dust particles can be modelled as spheroids in shape (Yang et al., 2007), a particular study of model errors in both spherical and spheroidal particles is carried out. Two different cases of the closure study for the microphysical-optical properties have been selected: the observations with influences of desert dust particles and those without this aerosol type. The classification method is reported in Sorribas et al. (2015a).

Table 2 shows the slope of the fits between the computed and observed scattering and backscattering properties for spherical and spheroid particles and the classification of non-desert and desert dust observations. The correlation coefficient (R) (not show in Table 2) ranges from

0.85 to 0.96 within the fine mode and from 0.70 to 0.83 within the coarse mode, evincing an agreement between the computed and observational data.

For particles with D < 1 μm, the differences for σ_{sp} and σ_{bsp} considering desert dust and non-desert dust are not large, thus allowing to conclude that the assumption of either spherical or spheroidal shapes within climate models for desert dust and non-desert dust cases would not cause a change in the observed findings.

For particles with 1 μm < D < 10 μm (coarse mode), the aerosol scattering and backscattering properties for both desert and non desert dust cases are better computed using the spheroid approximation, since the slope of the fit is closer to 1 for spheroidal particles. This could be caused by the usual particle shape within this size range, which is irregular with more angular and sharper edges (e.g. Pachauri et al., 2013).

The effect of the spheroid approximation on scattering and backscattering within the coarse mode was more distinct for desert dust aerosol than for non-desert days, especially for back-scattering. For example, Table 2 shows, for desert dust days and spherical particles, a slope of the fit of 0.49 (underestimation with a value of 51%) and 1.03 (overestimation of 3%) in the case of spheroidal particles. This represents a difference of 54% between both approximations. This difference for non-desert dust days was lower with a value of 36%. The explanation for such different behaviour most probably resides in the fact that the desert dust aerosol particles are more irregular than other coarse-mode aerosol particles at El Arenosillo, such as marine aerosols and secondary inorganic compounds (Sorribas et al, 2015a). Such chemical compounds are more spherical and the scattering properties computed by spheroidal approximation fit less than for desert dust compounds

Additionally, during desert dust days, the reduction of the computed backscattering underestimation was higher than the computed scattering underestimation. Therefore, the effect of the spheroid approximation was more severe on backscattering properties than on scattering properties. This can be explained because backscattering is more sensitive to particle shape (Bohren and Singham, 1991). A contributing factor for nephelometer measurements is that the scattering contains the backscattering data and hence, the scattering is also sensitive to particle shape, but less than the backscattering process.

4.2. Angular correction study

The angular correction proposed by Anderson and Ogren, (1998) is discussed in this section to explore its uncertainty in terms of size range and aerosol chemical compounds. The computed and observed σ_{sp} and σ_{bsp} values were compared under the assumption of light scattered over the full (0º-180º) angular range, considering the uncertainty in the light scattering measurement within the (0º-7º) and (170º-180º) angular ranges. As in Section 4.1., with similar refractive index values (m), the SMPS-APS number size distributions were used to compute the scattering coefficient by means of Mie and T-matrix theories at wavelengths 450 nm, 550 nm and 700 nm. Figure 1 represents the observed versus computed scattering and backscattering values within the (7º-90º) and (90º-170º) angular ranges, considering the nephelometer wavelength and angular sensitivities on the computed properties. Figure 2 shows similar data for the full (0º-180º) angular range (without nephelometer sensitivities on computed properties), while the Anderson and Ogren, (1998) correction was applied on the observed properties. The differences between Figures 1 and 2 make it possible to analyse the uncertainty of the angular correction for Anderson and Ogren, (1998). The main findings are:

For particles with D < 1 μm (fine mode):

(1) *Scattering coefficient*: comparing Figures 1a.2 and 2a.2 (at 550 nm), there is no high variation in the slope of the fit for sphere particles. No differences were also seen for spheroid particles. Therefore, for all wavelengths considered, it can be concluded that the angular correction underestimates the observed scattering for both spherical and spheroidal approximations by less than 3%.

(2) *Backscattering*: the correction yields an overestimation about 4% for the backscattering properties for spherical and spheroid particles. This is shown by the comparison between the slope of the fits in Figures 1b and 2b.

For particles with 1 μm < D < 10 μm (coarse mode):

(3) *Scattering coefficient*: comparison of Figures 1c.2 and 2c.2 shows that for spherical and spheroidal particles the angular correction overestimates the observed scattering by 8%. Then the error discussed for particle scattering within the coarse mode is higher than the error observed for scattering and backscattering within the fine mode.

(4) *Backscattering*: the slope of the fit varied from 0.47 (Figure 1d.2) to 0.49 (Figure 2d.2) for the spherical approximation, meaning an overestimation of the angular correction by 2%. For the spheroidal approximation the slope of the fit are similar. Therefore, the computed scattering and backscattering did not vary when de angular correction was applied.

All this information means that the angular correction proposed by Anderson and Ogren, (1998) can be applied with an error lower than -3% in σ_{sp}(D<1 μm), +4% in σ_{bsp}(D<1 μm) and +8% σ_{sp}(1 μm<D<10 μm) for spherical and spheroids particles. In case of the backscattering properties within the coarse mode, the errors discussed are +2% for both sphere and zero for

spheroidal particles. When the uncertainty of the angular correction factors for spherical particle provided by Anderson and Ogren is compared to our results, the largest differences are found in the scattering of the particles within the coarse mode. While the uncertainty is 28% at 550 nm in Anderson and Ogren, (1998), it is only 8% in our study. Discrepancies can be attributed to the differences in size and composition parameters, as Anderson and Ogren, (1998) used a broad range of refractive index values and coarse mode populations with a larger value of the modal diameter, as well as a fixed value of the fine/coarse mode particle ratio.

Table 3 shows the slope of the fits between the computed and observed scattering and backscattering properties, for spherical and spheroidal particles and whether the classification of the non-desert and desert dust observations is considered. The computed and observed σ_{sp} and σ_{bsp} were compared when the light was scattered at (0º-180º) angular range. The uncertainty in the light scattering measurement within the (0º-7º) and (170º-180º) angular ranges was considered. The correlation coefficient (R) (not show in Table 3) ranges from 0.85 to 0.96 within the fine mode and from 0.69 to 0.83 within the coarse mode, evincing an agreement between the computed and observational data.

The comparison of Tables 2 and 3 shows that, for the coarse mode, when the angular correction is applied under the spherical and spheroidal shape assumptions, the deviation in scattering is considerably larger during desert dust days with a value of ~13% (e.g. for scattering, difference between 0.56 (Table 2) and 0.69 (Table 3)). The other optical parameters show a deviation lower than 6%. Higher uncertainties for desert dust aerosol could be related to the uncertainty in modelling the spheroid geometry (axial ratio) and the particle composition (refractive index).

5. CONCLUSIONS

The uncertainty in studying the aerosol scattering process in the atmosphere due to the non-spherical nature of particles has been investigated. The goals have been to analyze the error associated with: (1) the computed scattering and backscattering properties when spherical and spheroid approximations are used and (2) the observed scattering using nephelometers due to the angular error. Mie theory and the T-matrix method have been applied to compute optical properties for spherical and spheroidal particles, using observed particle size distributions. The computed scattering and backscattering properties were represented versus the observed optical data for both fine and coarse modes, and the slope of each fit was analyzed.

For spherical and non-spherical particles the computations show that the scattering and backscattering coefficients are little influenced by the shape of the particles in the fine mode. Additionally, the computed backscattering values at 550 nm underestimate the observed values by ~15%. By contrast, the data indicate that the spheroidal approximation finds better results than the spherical particles assumption within the coarse mode, particularly for backscattering properties. Nonetheless, even after applying the spheroidal approximation, the computed scattering and backscattering values at 550 nm are underestimated 49% and 11%, respectively. This is mainly attributed to the characteristics (axial ratio and refractive index) used in this study for modelling the particle, and the uncertainty in the particle size distribution measurements. It was also concluded that scattering and backscattering within coarse mode are better computed for spheroidal approximation during days with desert dust present. The explanation for this conclusion resides in the fact that desert dust aerosol particles are more irregular than other aerosol in El Arenosillo. Additionally, backscattering was more sensitive to particle shape than was scattering during desert dust days.

The angular correction proposed by Anderson and Ogren, (1998) was also examined to explore its uncertainty depending size range and particle shape. In conclusion for particles within the fine

mode, the angular correction underestimates the observed scattering for both spherical and spheroidal approximations by less than ~3%. On the other hand an overestimation of about ~4% for the backscattering properties was found. For particles within the coarse mode, the uncertainty for scattering is about 8%. By contrast, in case of the backscattering properties, there is no influence of the angular correction.

Additionally, if spheroidal particles are used to evaluate the aerosol optical properties, the correction proposed by Anderson and Ogren, (1998) must be re-evaluated with the aim of reducing the uncertainty found when being applied for scattering within the coarse mode. This recommendation is for sites under the influence of desert dust aerosol, since the deviation from the computed scattering and backscattering values increases up to 13% for desert dust aerosol.

Acknowledgments – M. Sorribas thanks MINECO for the award of a postdoctoral grant (Juan de la Cierva). This work was partially supported by the Andalusian Regional Government through projects P10-RNM-6299 and P12-RNM-2409, by the Spanish Ministry of Science and Technology through projects CGL2010-18782, CGL2011-24891/CLI and CGL2013-45410-R, and by EU through ACTRIS project (EU INFRA-2010-1.1.16-262254). Technical support of NOAA/ESRL aerosol network by the nephelometer is gratefully acknowledged. We thank Dr. John Ogren to provide us the wavelength and angular corrections of the nephelometer by personal communication. Finally, we also thank Dr. Andrew Kowalski for revising the manuscript.

References

Adame, J.A., Martínez, M., Sorribas, M., Hidalgo, P.J., Harder, H., Diesch, J.-M., Drewnich, F., Song W., Williams, J., Sinha, V., Hérnadez-Ceballos, M. A., Vilâ-Guerau de Arellano, J., Sander, R., Hosaynali-Beygi, Z., Fischer, H., Lelieveld, J., De la Morena, B. 2014. Meteorology during

the DOMINO campaign and its connection with trace gases and aerosols. *Atmos. Chem. Phys.*, 14, 2325-2342, doi: 10.5194/acp-14-2325-2014.

Anderson, T. L., Covert, D. S., Marshall, S. F., Laucks, M. L., Charlson, R. J., Waggoner, A. P., Ogren, J. A., Caldow, R., Holm, R., Quant, F., Sem, G., Wiedensohler, A., Ahlquist, N. A., Bates, T. S. 1996. Performance characteristics of a high-sensitivity, three-wavelength, total scatter backscatter nephelometer. *J. Atmos. Oceanic Technol.*, 1996, 13, pp. 967-986.

Anderson, T.L., Ogren, J.A. 1998. Determining aerosol radiative properties using the TSI 3563 integrating nephelometer. *Aerosol Sci. Technol.*, 29:57–69.

Antón, M., Sorribas, M., Bennouna, Y., Vilaplana, J.M., Cachorro, V.E., Gröbner, J., Alados-Arboledas. 2012. Effects of an extreme desert dust event on th espectral ultravioleta irradiance at El Arenosillo (Spain). *J. Geophys. Res.*, 117, D03205, doi:10.1029/2011JD016645.

Bohren, C.F., Singham, S.B. 1991. Backscattering by nonspherical particles: A review of methods and suggested new approaches. *J. Geophys. Res.*, 96, 5269-5277, doi:10.1029/90JD01138.

Bond, T.C., Covert, D.S., Müller, T. 2009. Truncation and angular-scattering corrections for absorving aerosol in the TSI 3563 nephelometer. *Aerosol Sci. Technol.*, 43, 866-871.

Córdoba-Jabonero, C., Sorribas, M., Guerrero-Rascado, J.L., Adame, J.A.m Hernández, Y., Lyamani, H., Cachorro, V., Gil, M., Alados-Arboledas, L., Cuevas, E., De la Morena, B.A. 2011. Synergetic monitoring of Saharan dust plumes and potencial impact on surface: a case study of dust transport from Canary Islands to Iberian Peninsula. *Atmos. Chem. Phys.*, 11, 3067-3091.

Dubovik, O., B. N. Holben, T. Lapyonok, A. Sinyuk, M. I. Mishchenko, P. Yang, I. Slutsker. 2002. Non-spherical aerosol retrieval method employing light scattering by spheroids, *Geophys. Res. Lett.*, 29(10), 1415, doi:10.1029/2001GL014506.

Dubovik, O., Sinyuk, A., Lapyonok, T., Holben, B.N., Mishchenko, 435 M., Yang, P., Eck, T. F., Volten, H., Muñoz. O., Veihelmann, B., van der Zande, W. J., Leon J.-F., Sorokin, M., Slutsker, I. 2006. Application of spheroidal models to account for aerosol particle nonsphericity in remote sensing of desert dust. *J. Geophys. Res.*, D111, D11208, doi:10.1029/2005JD06619.

Guerrero-Rascado, J. L., Andrey, J., Sicard, M., Molero, F., Comerón, A., Pujadas, M., Rocadenbosch, F., Pedrós, R., Serrano-Vargas, O., Gil, M., Olmo, F.J., Lyamani, H., Navas-Guzmán, F., Alados-Arboledas, L. 2011. Aerosol closure study by lidar, Sun photometry, and airborne optical counters during DAMOCLES field campaign at El Arenosillo sounding station, Spain, *J. Geophys. Res.*, 116, D02209, doi:10.1029/2010JD014510.

Hand, J.L., Kreidenweis, S.M. 2002. A new method for retrieving particle refractive index and effective density from aerosol size distribution data. *Aerosol Sci. Technol.*, 36:10, 1012-1026.

Heintzenberg, J., Wiedensohler, A., Tuch, T.M., Covert, D.S., Sheridan P., Ogren, J.A., Gras, J., Nessler, R., Kleefeld, C., Kalivitis, N., Altonen, V., Wilhelm, R.-T., Havlicek, M. 2006. Intercomparisons and aerosol calibrations of 12 commercial integrating nephelometers of three manufactures. *J. Atmos. Oceanic Technol.*, 23, 902-914.

Hill, S.C., Hill, A.C., Barber, P.W. 1984. Light scattering by size/shape distributions of soil particle and spheroids. *Appl. Opt.*, 23, 1025-1031.

IPCC, 2014, IPCC Fifth Assessment Report Climate Change 2014 – The physical science basis contribution of working group to the fourth assessment report of the IPCC, ISBN 978-1-107-05799-1 Hardback; 978-1-107-66182-0 Paperback.

Kahnert, M., Nousiainen, T., Räisänen, P. 2007. Mie simulations as an error source in mineral aerosol radiative forcing calculations. *Q. J. R. Meteorol. Soc.*, 133, 299:307.

Klaver, A., Formenti, P., Caquineau, S., Chevaillier, S., Ausset, P., Calzolai, G., Osborne, S., Johnson, B., Harrison, M., Dubovik, O. 2011. Physico-chemical and optical properties of Sahelian and Saharan mineral dust : in situ measurements during the GERBILS campaign. *Q. J. R. Meteorol. Soc.*, 137, 1193-1210.

Lindqvist, H., Jokinen, O., Kandler, K., Scheuvens, D., Nousiainen, T. 2014. Single scattering by realistic, in homogeneous mineral dust particles with stereogrammetric shapes. *Atmos. Chem. Phys.*, 14, 143-157.

Massoli, P., Murphy, D.M., Lack, D.A., Baynard, T., Brock, C.A., Lovejoy, E.R. 2009. Uncertainty in light scattering measurements by TSI nephelometer: results from laboratory studies and implications for ambient measurements. *Aerosol Sci. Techonol.*, 43, 1064-1074.

Mie, G. 1908. Beiträge zur Optik trüber Medien, speziell kolloidaler Metallösungen. *Ann. d. Phys.* 25, 377-445.

Mishchenko, M. I., I. V. Geogdzhayev, L. Liu, J. A. Ogren, A. A. Lacis, W. B. Rossow, J. W. Hovenier, H. Volten, O. Muñoz. 2003. Aerosol retrievals from AVHRR radiances: Effects of

particle nonsphericity and absorption and an updated long-term global climatology of aerosol properties, *J. Quant. Spectrosc. Radiat. Transfer.*, 79/80, 953– 972.

Mishchenko, M. I., Travis, L. D. 1998. Capabilities and limitations of a current Fortran implementation of the T-matrix method for randomly oriented rotationally symmetric scatterers. *J. Quant. Spectrosc. Radiat. Transf.*, 60, 309–324.

Mishchenko, M. I., Travis, L. D., Kahn, R.A., West, R.A. 1997. Modelling phase functions for dislike tropospheric aerosols using a shape mixture or randomly oriented polydisperse spheroids. *J. Geophys. Res.*, D14, 16831-16847.

Mishchenko M.I. Light scattering by randomly oriented axially symmetric particles. 1991. .*J Opt. Soc. Am.,* A8, 871-882; Errata 9, 497.

Müller, T., Laborde, M., Kassell, G., Wiedensohler, A. 2011. Design and performance of a three-wavelenght LED-based total scatter and backscatter integrating nephelometer. *Atmos. Meas. Tech.*, 4, 1291-1303.

Pachauri, T., Singla, V., Satsangi, A., Lakhani, A., Kumari K.M. 2013. SEM-EDX Characterization of individual coarse particles in Agra, India. *Aerosol Air Qual. Res.*, 13, 523 - 536.

Prats, N., Cachorro, V.E., Sorribas, M., Mogo, S., Berjón, A., Toledano, C., De Frutos, A.M., De la Rosa, J. Laulainen, N., De la Morena, B.A. 2008. Columnar aerosol optical properties during 'El Arenosillo 2004 summer campaign'. *Atmos. Environ.*, 42, 11, 2643-2653.

Quirantes A, Olmo FJ, Valenzuela A, Lyamani H, Alados-Arboledas L. 2010. 'ALFA/BETA: A Dual Database for Light Scattering Simulations on Atmospheric Aerosols'. *In Proceedings of RECTA 2010 – IV Reunión Española de Ciencia y Tecnología del Aerosol, Granada, Spain.*

Quirantes, A., Olmo, F.J., Valenzuela, A., Lyamani, H., Alados-Arboledas, L. 2011. ALFA: A database for light scattering simulations with atmospheric aerosol applications. *Óptica Pura y Aplicada*, 44 (4), 641-645.

Raisanen, P., Haapanala, P., Chung, C.E., Kahnert, M., Makkonen, R., Tonttila, J., Nousiainen, T. 2013. Impact of dust particle non-sphericity on climate simulations. *Q. J. R. Meteorol. Soc.*, 139, 2222-2232.

Sorribas, M., De la Morena, B.A., Wehner, B., López, J.F., Prats, N., Mogo, S., Wiedensohler, A., Cachorro, V.E. 2011. On the sub-micron aerosol size distribution in a coastal-rural site at El Arenosillo Station (SW-Spain). *Atmos. Chem. Phys.*, 11, 11185-11206.

Sorribas, M., Ogren, J.A., Olmo, F.J., Quirantes, A., Fraile, R., Gil, M., Alados-Arboledas, L. 2015a. Assessment of African desert dust episodes over southwest Spain at sea level using in-situ aerosol optical and microphysical properties.. *Submitted to Tellus B.*

Sorribas, M., Adame, J.A., Olmo, F.J., Vilaplana, J.M., Gil, M., Alados-Arboledas, L. 2015b. Long-term study of new particle formation in a coastal environment: meteorology, gas phase and solar radiation implications. *Science and Total Environment*, 511, 723-737, 10.1016/j.scitotenv.2014.12.011.

Valenzuela, A., Olmo, F.J., Lyamani, H., Antón, M., Quirantes, A., Alados-Arboledas, L. 2012a. Aerosol radiative forcing during African desert dust events (2005-2010) over Southeastern Spain. *Atmos. Chem. Phys.*, 12, 10331-10351. http://dx.doi.org/10.5194/acp-12-10331-2012.

Valenzuela, A., Olmo, F.J., Lyamani, H., Antón, M., Quirantes, A. Alados-Arboledas, L. 2012b. Analysis of the columnar radiative properties retrieved during African desert dust events over Granada (2005-2010) using principal plane sky radiances and spheroids retrieval procedure. *Atmos. Res.*, 104-105, 292-301. http://dx.doi.org/10.1016/j.atmosres.2011.11.005

Valenzuela, A., Olmo, F.J., Lyamani, H., Antón, M., Quirantes, A., Alados-Arboledas, L. 2012c. Classification of aerosol radiative properties during African desert dust intrusions over southeastern Spain by sector origins and cluster analysis. *J. Geophys. Res.*, 117, D06214. http://dx.doi.org/10.1029/2011JD016885.

Wang, H.-C, Walter, J. 1987. Particle density correction for the Aerodynamic Particle Sizer. *Aerosol Sci. Technol.*, 6(2), 191-198.

Wiedensohler, A., Birmili, W., Nowak, A., Sonntag, A., Weinhold, K., Merkel, M., Wehner, B., Tuch, T., Pfeifer, S., Fiebig, M., Fjäraa, A. M., Asmi, E., Sellegri, K., Depuy, R., Venzac, H., Villani, P., Laj, P., Aalto, P., Ogren, J. A., Swietlicki, E., Williams, P., Roldin, P., Quincey, P., Hüglin, C., Fierz-Schmidhauser, R., Gysel, M., Weingartner, E., Riccobono, F., Santos, S., Grüning, C., Faloon, K., Beddows, D., Harrison, R., Monahan, C., Jennings, S. G., O'Dowd, C. D., Marinoni, A., Horn, H.-G., Keck, L., Jiang, J., Scheckman, J., McMurry, P. H., Deng, Z., Zhao, C. S., Moerman, M., Henzing, B., de Leeuw, G., Löschau, G., Bastian, S. 2012. Mobility particle size spectrometers: harmonization of technical standards and data structure to facilitate

high quality long-term observations of atmospheric particle number size distributions, *Atmos. Meas. Tech.*, 5, 657-685, doi:10.5194/amt-5-657-2012.

Willeke, K., Baron, P.A. 1993. *Aerosol measurements principles, techniques and applications*. Van Nostrand Reinhold, New York, USA, 143-195.

Yang P., Feng Q., Hong G., Kattawar G.W., Wiscombe W.J., Mishchenko M.I., Dubovik, O., Laszlo, I., Sokolik, I.N. 2007. Modeling of the scattering and radiative properties of nonspherical dust-like aerosols. *J. Aerosol Sci.*, 38, 995–1014.

TABLES

Table 1. Constants used to estimate the angular truncation correction for an integrated nephelometer (Anderson and Ogren, 1998).

	λ = 450 nm		λ = 550 nm		λ = 700 nm	
	a	b	a	b	a	b
D < 10 μm	1.365	-0.156	1.337	-0.138	1.297	-0.113
D < 1 μm	1.165	-0.460	1.152	-0.044	1.120	-0.035

Table 2 - The slope of the closure assessment fit of the scattering (σ_{sp}) and backscattering (σ_{bsp}) distributions at 450 nm , 550 nm and 700 nm , within the fine and coarse modes: observed vs. computed by the Mie Theory (spheres) and T-matrix Method (spheroids) during non-desert days and desert days. The observed optical parameters were calculated using the spectral and angular sensitivities of the nephelometer. The computed optical parameters were considered without the angular correction.

			Non-Desert		**Desert**	
Size range	*Optical Property*	*Wavelength*	*Spheres*	*Spheroids*	*Spheres*	*Spheroids*
Fine Mode	σ_{sp}	*450 nm*	0.92	0.89	0.97	0.93
		550 nm	0.88	0.85	0.93	0.90
		700 nm	0.83	0.80	0.89	0.87
	σ_{bsp}	*450 nm*	0.86	0.85	0.89	0.88
		550 nm	0.86	0.85	0.90	0.89
		700 nm	0.72	0.71	0.75	0.75
Coarse Mode	σ_{sp}	*450 nm*	0.41	0.46	0.47	0.57
		550 nm	0.44	0.48	0.50	0.56
		700 nm	0.50	0.53	0.56	0.61
	σ_{bsp}	*450 nm*	0.38	0.77	0.41	1.01
		550 nm	0.46	0.82	0.49	1.03
		700 nm	0.49	0.78	0.53	0.97

Table 3 - The slope of the closure assessment fit of the scattering (σ_{sp}) and backscattering (σ_{bsp}) distributions at 450 nm , 550 nm and 700 nm , within the fine and coarse modes: observed vs. computed by Mie Theory (spheres) and the T-matrix Method (spheroids) during non-desert days and desert days. The computed optical parameters were calculated in (0º-180º) angle range and observed parameters were considered with the angular correction.

			Non-Desert		**Desert**	
Size range	*Optical Property*	*Wavelength*	*Spheres*	*Spheroids*	*Spheres*	*Spheroids*
Fine Mode	σ_{sp}	*450 nm*	0.94	0.91	0.98	0.95
		550 nm	0.90	0.87	0.95	0.92
		700 nm	0.83	0.81	0.89	0.87
	σ_{bsp}	*450 nm*	0.89	0.87	0.92	0.90
		550 nm	0.90	0.87	0.94	0.92
		700 nm	0.74	0.73	0.78	0.77
Coarse Mode	σ_{sp}	*450 nm*	0.47	0.53	0.59	0.72
		550 nm	0.49	0.54	0.63	0.69
		700 nm	0.54	0.58	0.70	0.74
	σ_{bsp}	*450 nm*	0.40	0.76	0.43	0.99
		550 nm	0.48	0.81	0.52	1.01
		700 nm	0.51	0.77	0.56	0.97

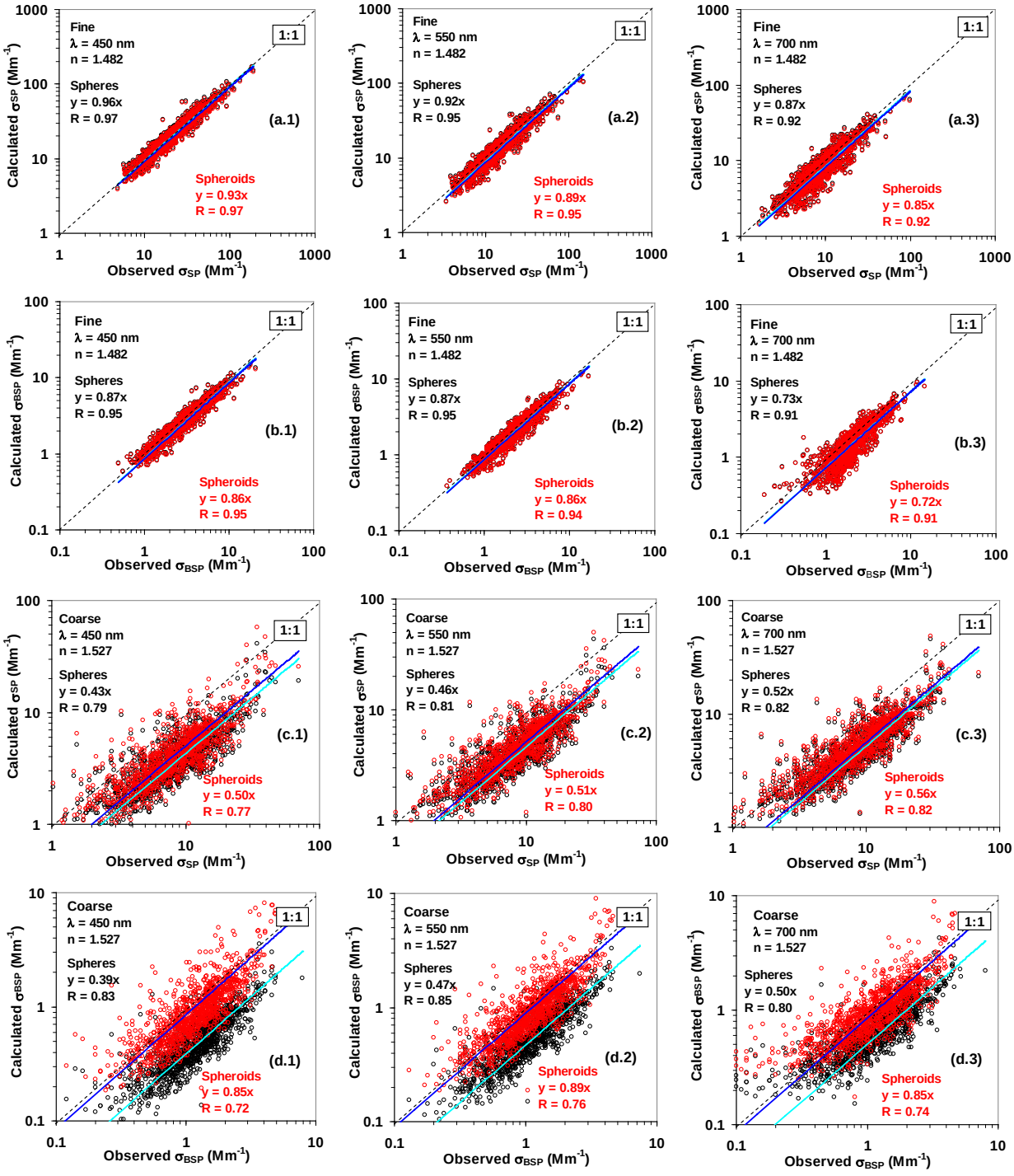

Figure 1 - A closure assessment of the optical data obtained with the integrating nephelometer: observed vs. computed scattering (Figures a and c) and backscattering (Figures b and d) by Mie Theory (black points) and the T-matrix (red points). The computations are based on fine (D_a<1 μm) and coarse size range (1 μm <D_a<10 μm) at 450, 550 and 700 nm. The 1:1 line is the dashed line. In each panel, the size range, the nephelometer wavelength, the refractive index, the slopes of the fits and the R correlation coefficient are shown. The fit for spheres is in light blue and that for spheroids is in dark blue. The observed optical parameters were calculated using the spectral and angular sensitivities of the nephelometer. The computed optical parameters were considered without the angular correction.

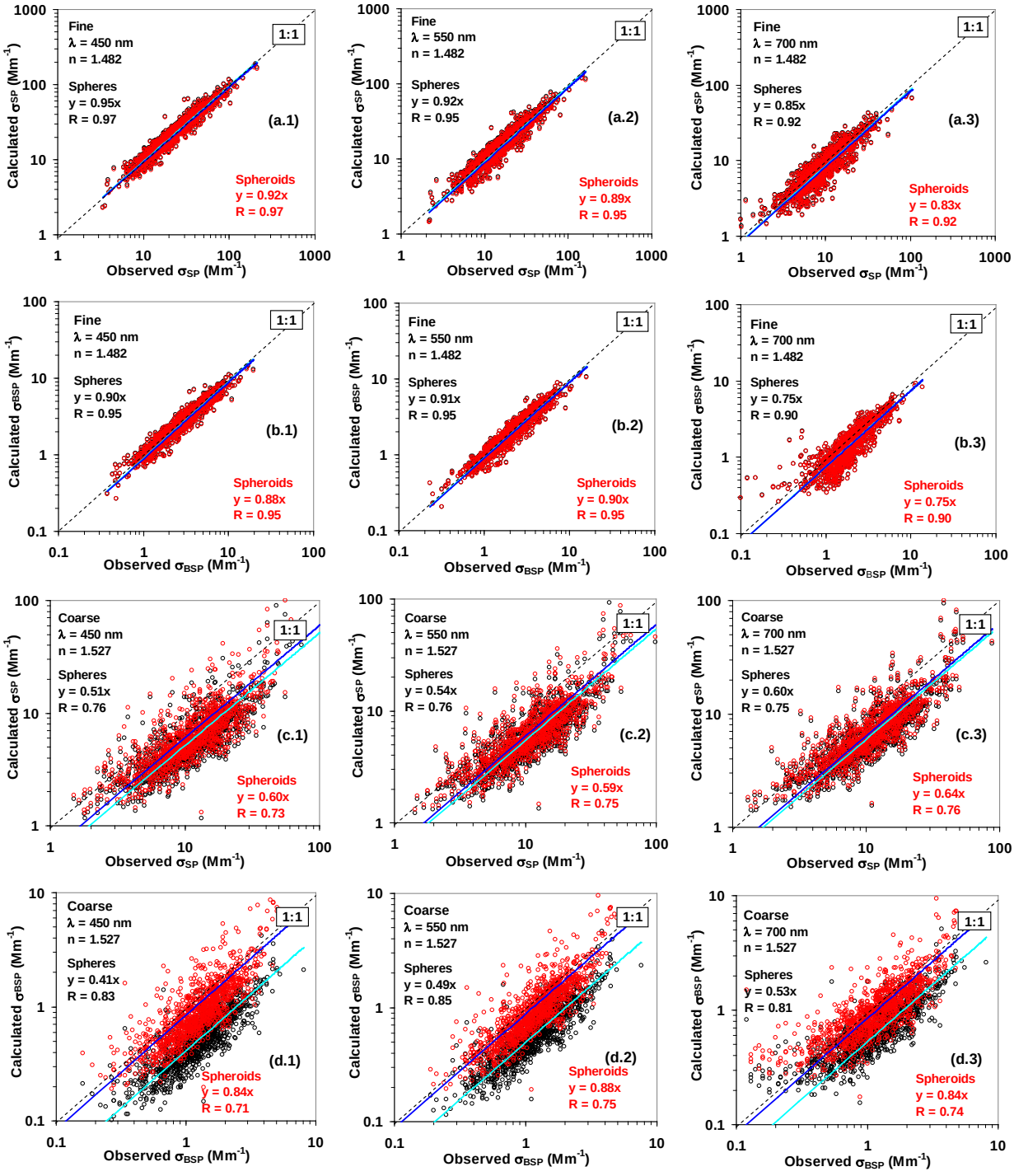

Figure 2 - A closure assessment of the optical data obtained with the integrating nephelometer: observed vs. computed scattering (Figures a and c) and backscattering (Figures b and d) by Mie Theory (black points) and the T-matrix (red points). The computations are based on fine (D_a<1 μm) and coarse size range (1 μm <D_a<10 μm) at 450, 550 and 700 nm. The 1:1 line is the dashed line. In each panel, the size range, the nephelometer wavelength, the refractive index, the slopes of the fits and the R correlation coefficient are shown. The fit for spheres is in light blue and that for spheroids is in dark blue. The computed optical parameters were calculated in (0º-180º) angle range and observed parameters were considered with the angular correction.